Microlasers based on effective index confined slow light modes in photonic crystal waveguides

Samuele Gardin[1,2], Frederic Bordas[1], Xavier Letartre[1], Christian Seassal[1], Adel Rahmani[3], Renato Bozio[2], Pierre Viktorovitch[1]

1 Université de Lyon, Institut des Nanotechnologies de Lyon-INL, UMR CNRS 5270, Ecole Centrale de Lyon, 36 Avenue Guy de Collongue, F-69134 Ecully, France
2 Chemistry Department, University of Padova, and INSTM, Via Marzolo 1, I-35131 Padova, Italy
3 Department of Mathematical Sciences and CUDOS, University of Technology, Sydney NSW 2007, Australia
Email: Christian.Seassal@ec-lyon.fr

Abstract: We present the design, theory and experimental implementation of a low modal volume microlaser based on a line-defect 2D-photonic crystal waveguide. The lateral confinement of low-group velocity modes is controlled by the post-processing of 1 to 3µm wide PMMA strips on top of two dimensional photonic crystal waveguides. Modal volume around 1.3 $(\lambda/n)^3$ can be achieved using this scheme. We use this concept to fabricate microlaser devices from an InP-based heterostructure including $InAs_{0.65}P_{0.35}$ quantum wells emitting around 1550nm and bonded onto a fused silica wafer. We observe stable, room-temperature laser operation with an effective lasing threshold around 0.5mW.

OCIS codes: (140.3948) Microcavity devices; (130.5296) Photonic crystal waveguide.

References and links

1. M. Imada, A. Chutinan, S. Noda, and M. Mochizuki, "Multidirectionally distributed feedback photonic crystal lasers," Phys. Rev. B **65**, 195306, 2002.
2. C. Monat, C. Seassal, X. Letartre, P. Regreny, M. Gendry, P. Rojo-Romeo, P. Viktorovitch, M. Le Vassor d'Yerville, D. Cassagne, et J. P. Albert, E. Jalaguier, S. Pocas, and B. Aspar, "InP-based two-dimensional photonic crystal on silicon: In-plane Bloch mode laser," Appl. Phys. Lett. **81** 5102-5104 (2002).
3. A. Sugitatsu and S. Noda, "Room temperature operation of a two dimensional photonic crystal slab defect-waveguide-laser with optical pump," Electron. Lett. **39**, 123-125 (2003).
4. Y. Akahane, T. Asano, B. S. Song, and S. Noda, "High-Q photonic nanocavity in a two-dimensional photonic crystal," Nature **425**, 944-947 (2003).
5. E. Kuramochi, M. Notomi, S. Mitsugi, A. Shinya, T. Tanabe, and T. Watanabe, "Ultrahigh-Q photonic crystal nanocavities realized by the local width modulation of a line defect," Appl. Phys. Lett **88**, 041112 (2006).
6. F. Bordas, M. J. Steel, C. Seassal, A. Rahmani, "Confinement of band edge modes in Photonic Crystals," Opt. Express **15**, 10890-10902 (2007), http://www.opticsinfobase.org/abstract.cfm?URI=oe-15-17-10890.
7. F. Bordas, C. Seassal, E. Dupuy, P. Regreny, M. Gendry, M. J. Steel, and A. Rahmani, "Room-Temperature InAs/InP Quantum-Dot Photonic Crystal Microlasers Using Cavity-Confined Slow Light," CLEO/QELS May 7-11 2007, Baltimore.
8. M. H. Shih, W. Kuang, A. Mock, M. Bagheri, E. H. Hwang, J. D. O'Brien, and P. D. Dapkus, "High-quality-factor photonic crystal heterostructure laser," Appl. Phys. Lett. **89**, 101104 (2006).
9. S. Tomljenovic-Hanic, C. M. de Sterke, M. J. Steel, B. J. Eggleton, Y. Tanaka and S. Noda, "High-*Q* cavities in multilayer photonic crystal slabs," Opt. Express **15**, 17248-17253 (2007), http://www.opticsinfobase.org/abstract.cfm?URI=oe-15-25-17248.
10. S. G. Johnson and J. D. Joannopoulos, "Block-iterative frequency-domain methods for Maxwell's equations in a planewave basis," Opt. Express **8**, 173-190 (2001), http://www.opticsinfobase.org/abstract.cfm?URI=oe-8-3-173.
11. B. S. Song, T. Asano, and S. Noda, "Physical origin of the small modal volume of ultra-high-Q photonic

#91883 - $15.00 USD Received 18 Jan 2008; revised 12 Mar 2008; accepted 14 Mar 2008; published 21 Apr 2008

double-heterostructure nanocavities," New J. Phys. **8**, 209 (2006).
12. M. Charbonneau-Lefort, E. Istrate, M. Allard, J. Poon, and E. H. Sargent, "Photonic crystal heterostructures: Waveguiding phenomena and methods of solution in an envelope function picture," Phys. Rev. B **65**, 125318 (2002).
13. http://alioth.debian.org/projects/tessa/.
14. C. Seassal, C. Monat, J. Mouette, E . Touraille, B. Ben Bakir, H. Hattori, J. L. Leclercq, X. Letartre, P. Rojo-Romeo, and P. Viktorovitch, "InP bonded membrane photonics components and circuits: Toward 2.5 dimensional micro-nano-photonics," IEEE J. Sel. Top. in Quantum Electron. **11**, 395-407 (2005).
15. X. Letartre, C. Monat, C. Seassal, and P. Viktorovitch, "An analytical modeling and an experimental investigation of 2D Photonic Crystal Micro-lasers : defect state (micro-cavity) versus band edge state (distributed feed-back) structures," J. Opt. Soc. Am. B **22**, 2581-2595 (2005).

1. Introduction

Over the past few years, various strategies have been proposed to devise resonators that exhibit both high Q-factors and low modal volume. One of the most promising approaches relies on the control of slow light modes in 2D photonic crystal (PC) slabs. Such modes, including band-edge modes of 2D PC membranes [1,2], and low group velocity modes in waveguides based on line defects in 2D PC [3] have already been used to demonstrate microlasers. However, the lateral extension of these modes is not controlled but rather limited by the losses, and therefore, the effective mode volume is far from optimal. More recently, different strategies were proposed in order to maximize and control the spatial confinement of such slow light modes. A first option consists in modifying locally of the position or size of the PC holes. This concept was applied to W1 waveguides (one missing row of holes along the Γ-K direction of a triangular lattice) by various groups [4,5], and more recently by some of the authors in the case of band-edge modes in triangular lattice 2D PCs [6]. In both cases, Q-factors in excess of 10^6 are achievable provided that the boundaries of the resonator are carefully adjusted. It has recently been demonstrated that lasing can be achieved using such designs [7,8].

We propose to achieve such a lateral confinement using a different implementation. The basic structure is an InP-based heterostructure, including a multi-quantum well region and bonded onto a fused silica wafer. A 2D PC with a W1 defect waveguide is first patterned in this structure. In a second step, a thin, transparent layer of polymethyl methacrylate (PMMA) is deposited on top, and then laterally patterned to yield a small dielectric strip on top of the PC structure, as schematically presented in Fig. 1 (structure called W1+PMMA).

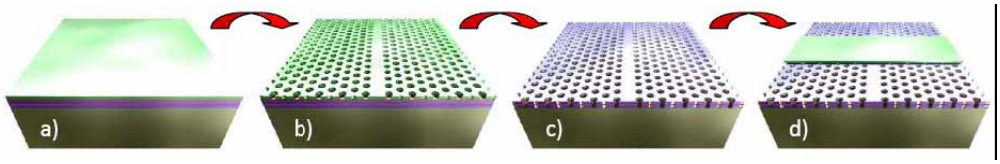

Fig. 1. Schematic representation of the experimental procedure necessary to obtain the W1+PMMA structure: (a) A 110 nm thick resist film is spin-coated on the sample surface; (b) the PC W1 structure is realized on the resist by Electron Beam Lithography (EBL) and then c) is transferred on the InP layer by means of Reactive Ion Etching (RIE); finally d) a PMMA strip is patterned above the PC with EBL.

#91883 - $15.00 USD Received 18 Jan 2008; revised 12 Mar 2008; accepted 14 Mar 2008; published 21 Apr 2008

2. Design and modeling

Figure 2(a) displays the band structure of a W1 waveguide calculated by the 3D plane-wave expansion method [10], and particularly the portion of the odd o_{g1} and even e_{g1} guided modes located under the light line (the even and odd modes are discriminated according to their symmetry with respect to the mirror plane perpendicular to the InP slab and parallel to the waveguide). The PC structure is designed to exploit the low group velocity mode located around point A of Fig. 1(a), at the edge of the first Brillouin zone. If one increases locally the effective index of the membrane, the bands are shifted to lower values of the reduced frequency, see Fig. 2(b).

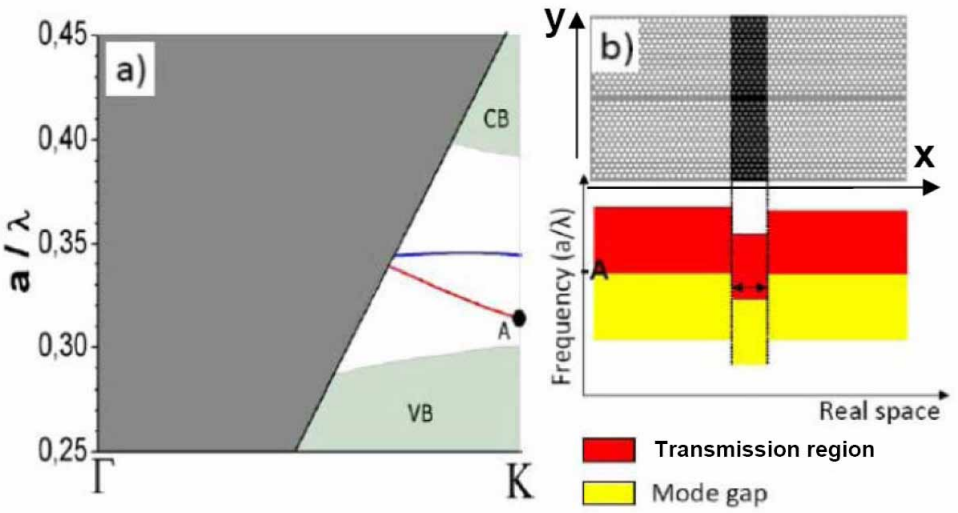

Fig. 2. (a) Calculated band diagram for the 2D photonic crystal slab with a triangular lattice and containing a line defect formed by a missing row of air holes. The dark grey area corresponds to the light cone, while the green zones correspond to the conduction and valence bands. The blue curve is the odd guided mode, while the red one corresponds to the even mode. (b) The PMMA strip over the PC waveguide locally lowers the energy of the waveguided mode creating a band gap: photons with this lower energy are trapped inside the region under the PMMA strip.

This results in a photonic heterostructure whose confinement properties are the result of the effective index shift and the local curvature of the band associated with the waveguide mode. The confinement properties of this type of cavity was explained by Song et al. by looking at the complex dispersion relation of the W1 waveguide using an analytic continuation of the wave vector [11]. Some of the confinement properties of the heterostructure can also be understood qualitatively using an envelope formalism inspired by the work of Charbonneau-Lefort et al. [12], which adapts the formalism originally applied to electrons in a perturbed periodic lattice to the case of optical modes inside a photonic heterostructure. The envelop is calculated using a simple 1D model of an infinite photonic crystal structure, where the optical confinement is controlled by the dielectric strip in a perturbative way. Although it cannot replace the rigorous, 3D FDTD computation that we present in the remainder of the article, the envelope picture provides a nice and simple illustration of the interplay between the geometric parameters of the waveguide and their influence on the confinement of the electric field.

In our case, we obtain an envelope equation which is expressed below:

#91883 - $15.00 USD Received 18 Jan 2008; revised 12 Mar 2008; accepted 14 Mar 2008; published 21 Apr 2008

$$\frac{1}{2m^*}\frac{d^2 f_{nk_0}(x)}{dx^2} = \left[\omega_n^2(k_0) - \omega_\lambda^2\left[1+\Delta(x)\right]\right] f_{nk_0}(x) \tag{1}$$

where m* is an effective-mass-like term, describing the curvature of the band.

This term is called effective mass by analogy with the effective mass of electrons in a periodic potential. ω_n and k_0 are the frequency and wave vector of the unmodified waveguide (edge of the first Brillouin zone), ω_λ the frequency of the confined mode, and Δ a factor linked to the effective index difference between the central region and the mirror region. The solution of this equation for a constant value of Δ, which is appropriate for our heterostructure, is obtained by application of the continuity conditions at the boundaries of the region delimited by the dielectric strip:

$$f_{nk_0} = \left\{ \begin{array}{c} \cos Kx \\ e^{\gamma\left(\frac{L}{2}-|x|\right)}\cos K\frac{L}{2} \end{array} \right\} if \left\{ \begin{array}{l} |x| < \frac{L}{2} \\ |x| > \frac{L}{2} \end{array} \right\} \tag{2}$$

with

$$K = \sqrt{2m^*\left(\omega_\lambda^2(1+\Delta(x)) - \omega_n^2(k_0)\right)} \tag{3}$$

and

$$\gamma = \sqrt{2m^*\left(\omega_n^2(k_0) - \omega_\lambda^2\right)} \tag{4}$$

The effective mass m* is the second derivative with respect to the parallel component of the wave vector of the frequency squared. It is linked to the curvature of the band α through the relation:

$$\frac{1}{m^*} = \left.\frac{\partial^2 \omega_n^2}{\partial k_x^2}\right|_{k_0} = 2\omega_0\alpha \tag{5}$$

This equation shows that the effective mass is inversely proportional to the band curvature. From the equations above, we can conclude that the efficiency of the confinement is higher for slow Bloch modes than for conventional (fast) modes, because the lower the band curvature, the better the spatial confinement. As can be seen in the equations, the size of the strip (L) and the effective index difference (Δ) also play a role in the confinement efficiency. If the effective index difference is small, L has to be large enough to obtain an efficient confinement within the PC region covered by the strip. On the other hand, if Δ is high, the cosine function oscillates faster and efficient lateral confinement can be achieved with a narrower strip. To summarize the physics of slow Bloch modes localization, the smaller the band curvature, the better the confinement. Furthermore there is a compromise between the size of the strip and the effective index difference between the covered and uncovered regions of the W1 waveguide. Figure 3 shows three calculated envelopes to illustrate the interplay between Δ and L. From the band diagram of the W1 waveguide, we estimate the unmodified waveguide frequency to be ω_n=0.31235 and the effective mass to be $m^*=7.34\times10^{-19}$ $m^{-2}s^2$. We also estimate the value of Δ from the change in effective index induced by the PMMA deposition to be Δ=0.06. The mode frequency obtained from these parameters is quite uniform across different heterostructure sizes L: ω_λ=0.3123 c/a for L=4a and ω_λ=0.3121 c/a for L=10a. The first envelope on Fig. 3 (black solid line) is calculated for L=4a, whereas the second one

#91883 - $15.00 USD Received 18 Jan 2008; revised 12 Mar 2008; accepted 14 Mar 2008; published 21 Apr 2008

(red dashed line) is calculated for L=10a. The third and last one (blue dash and dotted line) is calculated for L=4a also, but with a value of Δ hypothetically obtained from a high index material instead of the PMMA : Δ=0.1. The calculated frequency with this parameter is ω_λ=0.3099 c/a. So this Fig. illustrates the interplay between Δ and L: the increase of one of either of these parameters reduces the width of the envelope. For rigorous and quantitative analysis, we now model the full 3D structure.

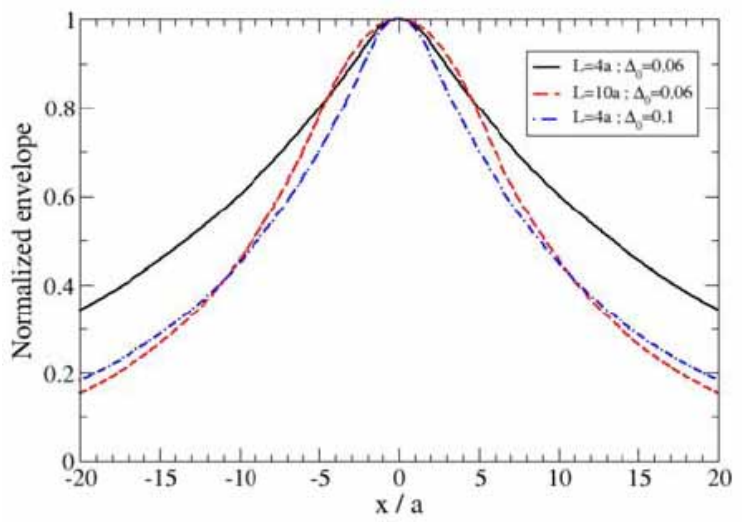

Fig. 3. Calculation of envelopes in the (x,z) plane at the middle of the waveguide for three different configurations (see text) extending from –20a to +20a.

Using the TESSA 3D Finite Difference in Time Domain (FDTD) open-source software [13], we modeled a W1 waveguide patterned in a 250 nm thick InP membrane, including a PMMA strip above. The lattice parameter and filling factor (respectively 473 nm and 40%) were chosen in such a way that the band-edge mode corresponding to point A of Fig. 2(a) stands around 1550 nm. Figure 4(a) shows the calculated spectrum for the W1 waveguide including a 6 period large PMMA strip laying across the waveguide. The waveguide was excited with a Gaussian dipole source centered at 1550 nm. The calculated spectrum shows two main peaks at 1494 and 1607 nm, corresponding to the odd o_{g1} and even e_{g1} modes at K point respectively.

The quality factors of the two modes are 771 and 4273 respectively. The Q factors of these modes would be much higher in the case of a suspended membrane, which offers a higher refractive index contrast between the InP slab and the surrounding media. However, since our goal is to develop stable non linear devices like microlasers, we chose to pattern a PC structure on an InP-based heterostructure bonded onto fused silica, which is mechanically stable, and exhibits a much better thermal behavior. In the case of our asymmetric structure, radiated losses of such resonant modes are therefore relatively high. However, as we will see, despite these losses, room-temperature lasing can be achieved.

#91883 - $15.00 USD Received 18 Jan 2008; revised 12 Mar 2008; accepted 14 Mar 2008; published 21 Apr 2008

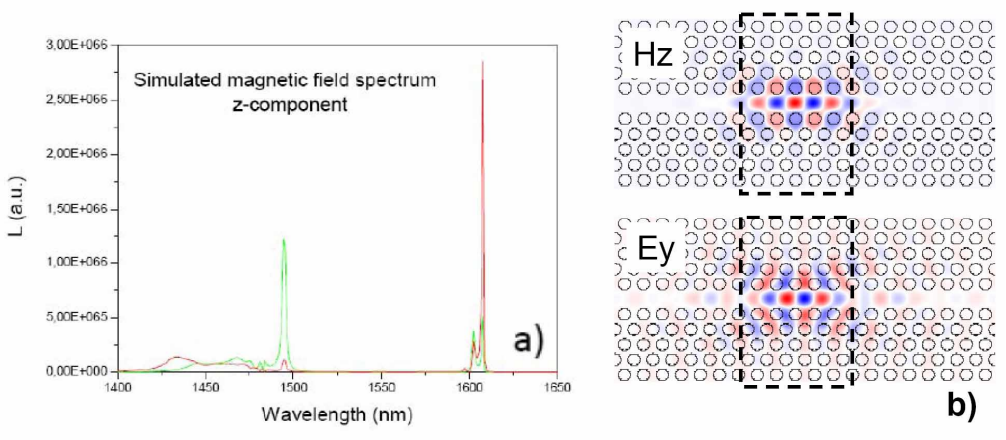

Fig. 4. Simulated H_z field spectrum (a) and (b) map of the e_{g1} mode at 1607 nm for the W1+PMMA configuration, the dashed rectangles correspond to the location.of the PMMA strip.

Figure 4(b) shows the simulated magnetic (z-component) and electric (y-component) field map for the mode at 1607nm. This Fig. clearly shows that this mode is well localized inside the waveguide region under the PMMA strip and this leads to a modal volume of the mode of only 1.31 $(\lambda/n)^3$, which means that the resonant mode is effectively concentrated at the center of the cavity. Under optimal conditions of spatial and spectral overlap between a source and the cavity mode, this cavity would exhibit a Purcell Factor of about 250.

3. Fabrication of the samples and optical characterization

The basic III-V semiconductor hetrostructure was grown by solid-source molecular beam epitaxy (MBE). It consists in a 250 nm thick InP membrane with a multi-quantum well region including four 50 Å thick $InAs_{0.65}P_{0.35}$ quantum wells, separated by 200 Å thick InP barriers. The heterostructure was then transferred onto a fused silica substrate by molecular bonding, and the InP substrate was removed by wet etching [14]. In order to pattern the photonic structure, a 90 nm thick SiO_2 layer was deposited over the InP membrane. The holes, together with alignment marks, were first defined by electron beam lithography with a modified JEOL (JSM5500) scanning electron microscope on a PMMA resist film, and then transferred into the SiO_2 layer using a CHF_3 based reactive ion etching (RIE). Finally, the pattern was transferred to the III-V heterostructure by RIE, using a gas mixture of CH_4 and H_2. Then, after the removal of the SiO_2 mask, in a second lithography step, a 6 periods wide and 110 nm thick strip of PMMA was patterned perpendicularly to the W1 waveguide across the entire PC width, with an accuracy on the order of 100 nanometers. Fig. 5 shows SEM images of a W1 waveguide and of the final structure.

In terms of lateral patterning, the big advantage of this confinement geometry is the great simplicity of the process, which requires less extreme technological equipment with respect to other configuration that requires nanometer-scale accuracy [4,5].

#91883 - $15.00 USD Received 18 Jan 2008; revised 12 Mar 2008; accepted 14 Mar 2008; published 21 Apr 2008

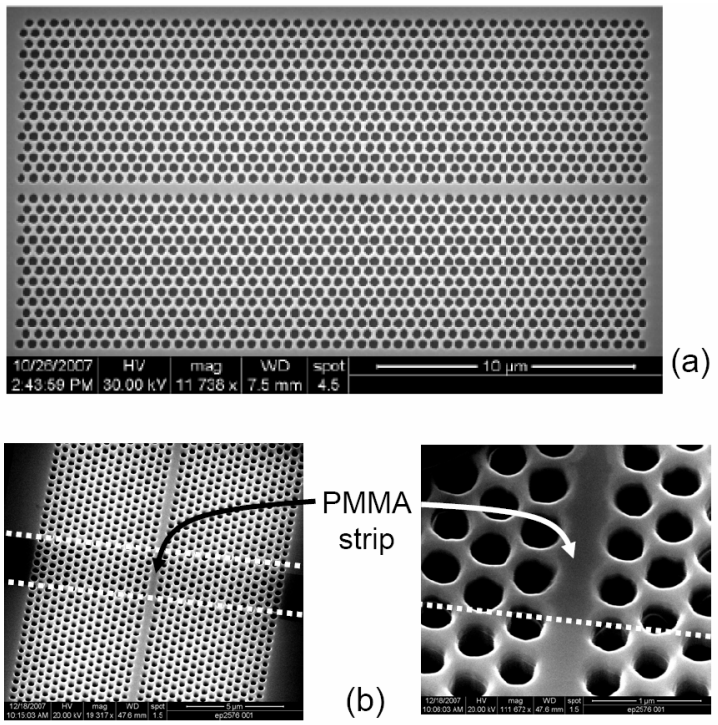

Fig. 5. SEM image of the W1 waveguide (a) and of the W1+PMMA cavity (b). The lattice period and hole radius are 478 nm and 154 nm respectively.

These active photonic structures were characterized at room temperature under pulsed optical pumping at 780 nm, with a pulse width of 7 ns and a 6 % duty cycle. The pumping beam was focused using a 20x microscope objective lens. The light emitted above the sample was collected through the same objective, and analyzed by a spectrometer, with spectral resolution around 0.1 nm. On Fig. 6(a), the emission spectrum of the unpatterned heterostructure (brown line), and four W1+PMMA structures, with small differences in the hole diameter, are shown. The photoluminescence spectrum of the unpatterned heterostructure covers a spectral range from 1400 to 1600 nm. The spectra of the patterned structures, measured with a pumping power of a few milliwatts, show a sharp and intense peak, corresponding to the e_{g1} mode at point A of Fig. 2(a). The variation of the peak intensity as a function of the incident peak pump power is displayed in Fig. 6(b), for both W1 and W1+PMMA structures. From these experimental data, we can conclude that the W1+PMMA structure exhibits a clear signature of lasing, with a threshold around 1.6 mW. Considering that only ~35% of the incident light is absorbed by the InP barriers, this leads to en estimate of the effective lasing threshold of 0.55 mW. For the W1 configuration, the lasing threshold has not been reached for the pumping energy range explored, possibly because the pumped area (~3 μm) is much less than the effective volume of the slow Bloch mode [15]. Figure 6(b) (inset) shows the emitted peak relative to the W1 and W1+PMMA configuration: the shift to longer wavelength of the emission peak in the W1+PMMA configuration can be observed, consistent with our theoretical prediction.

#91883 - $15.00 USD Received 18 Jan 2008; revised 12 Mar 2008; accepted 14 Mar 2008; published 21 Apr 2008

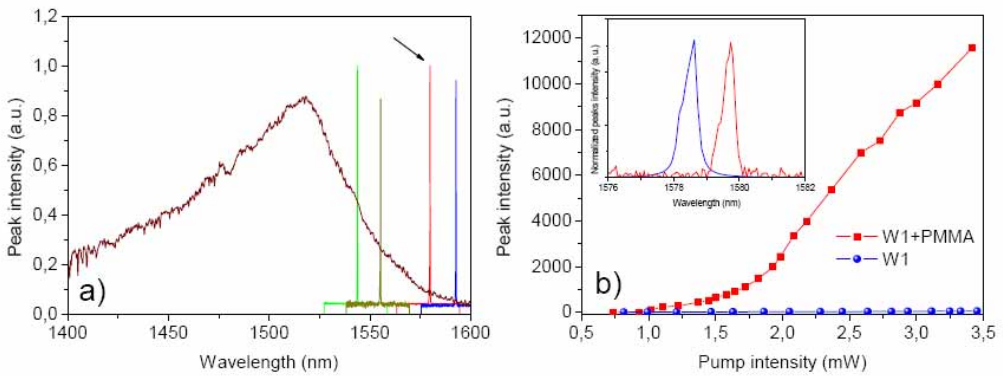

Fig. 6. (a) Spectrum of the spontaneous emission (brown line) and of the resonant peaks of four different structures (small changes in the holes radius). (b) laser intensity plotted against the incident pump power (7 ns pulse, 6% duty cycle) for one of the structures (indicated with the black arrow). The inset shows the peaks shape for the W1 (blue) and W1+PMMA (red) structures below lasing threshold.

To evaluate the effect of the cavity width, we performed a second set of measurements, using a PMMA strip with a width of about 1 μm. The effective modal volume for this cavity, obtained from the simulation, is around 1.29 $(\lambda/n)^3$, nearly the same as for the 3 μm wide PMMA strip; the corresponding Purcell Factor is about 135. Figure 7 shows the light out versus light in curve obtained for this configuration. From these curves one can see that the lasing threshold remains largely unchanged, as expected, given the nearly unchanged mode volume [14]. The main change is the increase of the slope efficiency, probably due to a higher directivity of the emission and therefore a better coupling to the collection optics.

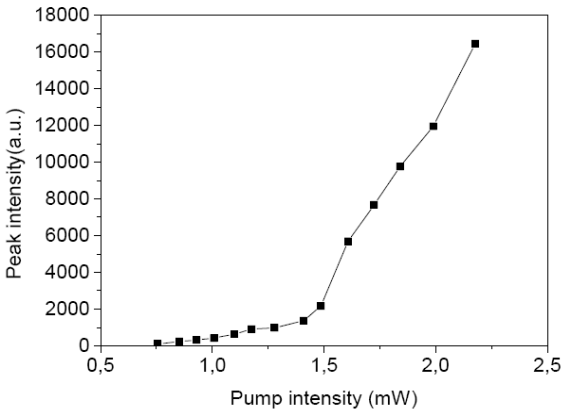

Fig. 7. Power in versus power out curve showing the power at the laser wavelength versus the incident pump power. The width of the PMMA strip is around 1 μm, and the pump pulse is around 7 ns long (6% duty cycle).

4. Conclusion

In this paper, we proposed, studied theoretically, and demonstrated a small mode volume, photon confinement scheme in an active microcavity. We achieved efficient spatial optical confinement using a local effective index modulation in a W1 PC waveguide supporting a low group velocity mode at the edge of the first Brillouin zone. The physics of the confinement has been explained through a simple model based on the envelope formalism. We fabricated

#91883 - $15.00 USD Received 18 Jan 2008; revised 12 Mar 2008; accepted 14 Mar 2008; published 21 Apr 2008

first test devices, comprising a W1 PC waveguide and a dielectric strip, on an InP-based multi-quantum well heterostructure bonded onto fused silica. The index modulation was achieved by electron beam patterning of a PMMA strip above the PC, which created a local increase of the effective index of the waveguide. Optical measurements have been performed on our structures and reproducible results have been obtained in agreement with the theoretical predictions. Laser emission was obtained with W1+PMMA structures at room temperature, with an estimated effective threshold of about 0.5 mW with PMMA strips 1 and 3μm wide. The simple and reproducible production process, together with the robustness and mechanical stability of the device, make this type of low threshold lasers good candidates for both surface-emitting or coupled-to-waveguide laser devices. Moreover the high Purcell Factor of 250 for the 3 μm wide PMMA strip, could lead to applications in the field of integrated quantum photonics. Finally, we emphasize that by changing the shape of the dielectric layer, other types designs for cavity-confined slow light modes can be fabricated in a similar fashion [6].

Acknowledgments

P. Regreny, from INL, is acknowledged for epitaxial growth of the InP-based heterostrtuctrure, and J.M. Fedeli and L. Di Cioccio, from CEA-LETI, for the wafer bonding technology. This work was partly performed in the framework of the EU FP6-ePIXnet network of excellence. CUDOS is an Australian Research Council Centre of Excellence.

#91883 - $15.00 USD Received 18 Jan 2008; revised 12 Mar 2008; accepted 14 Mar 2008; published 21 Apr 2008